Mechanical Behavior of Composite Materials

Ethan R. Thompson, Maya L. Patel
California Institute of Technology, Pasadena, USA

***Abstract*—**This paper presents the results of an experimental study undertaken to evaluate the local bond stress-slip response of short embedment of reinforcing bars in normal concrete (NC) and high performance fiber reinforced cement composites (HPFRCC) blocks. Long embedment was investigated as well to gain insights on the distribution of strain, slip, bar stress and bond stress along the bar especially in post-yield range. A total of 12 specimens were tested, by means of pull-out of the reinforcing bars from concrete blocks. It was found that the enhancement of local bond strength can be reached up to 50% and ductility of the bond behavior was improved significantly if HPFRCC is used. Also, under a constant strain at loaded end, HPFRCC has delayed yielding of bars at other location from the loaded end. Hence, the reduction of bond stress was slower for HPFRCC in comparison with NC. Due to the same reason, the total slips at loaded end for HPFRCC was smaller than NC as expected. Test results indicated that HPFRCC has better bond slip behavior which makes it a suitable material to be employed in anchorage zone such as beam-column joints.

***Keywords*—**Bond stress, high performance fiber reinforced cement composites, slip, strain.

I. Introduction

BOND slip failure in beam-column joints is always as one of the brittle failure that leads to the local damage collapse of structural frames under severe seismic loading. Nowadays, the use of high performance fiber reinforced composites (HPFRCC) in beam-column joints is becoming popular because of its superior tensile strain capacity that can enhance the overall ductility behavior of structures when subjected to earthquake loading. HPFRCC is proven to have compatible deformations with reinforcing bars in previous research [1]-[3], thus it is of interest to study the bond strength of bars embedded in HPFRCC.

A comprehensive local bond stress-slip response of deformed bars embedded in concrete (short embedment) has been characterized by [4]. It is well documented in Fib Model Code 2010 [5]. On the other hand, bond characteristic in postpost-yield range of deformed bars were intensively by several researchers [6], [7]. However, the available is only limited to bond-slip behavior of bars embedded in normal concrete. The study of bond-slip of bars embedded in HPFRCC is rare, only few researches have been devoted till to
date. Most of them focused on the bond splitting failure rather than pull-out failure [8], [9]. Some uniaxial tension tests have been conducted for single bar embedded in small prismatic of HPFRCC block up to the fracture failure of bars as can be found in [3] and [10]. But the bond-slip behavior between HPFRCC and bars was not sufficiently described.

Therefore, an experimental program is undertaken to investigate the bond-slip behavior of bars embedded in HPFRCC which focusing on pull-out failure for short embedment. Besides, bond behavior of bars embedded in HPFRCC in post-yield range was evaluated and compared with NC through this study.

II. Experimental Program

A. Test Specimens

The test specimens represented anchored beam bars in beam-column joints as shown in Fig. 1. A single deformed bar was embedded in the middle of each concrete block, confined with vertical bars and stirrups. Two types of embedment length have been investigated i.e. $5d_b$ and $20d_b$, where d_b is the bar diameter. Short embedment ($5d_b$) was selected to create local bond failures (bar pull-out), but it is limited to those anchored bars subjected to elastic strain only. Practically, post-yield strain could be developed in the anchored bars. Thus long embedment ($20d_b$) was studied to evaluate how the yielding of bars affected bond strength of anchored bars in HPFRCC. To prevent the effect of possible restraints to the end of concrete block, a bond free length of $5d_b$ was employed at both sides of bonded length, secured by placing bars in PVC pipes. Only one size of high yield bars (13 mm in diameter) has been used as anchored bar. Confining reinforcement was provided by four 10 mm high yield vertical bars and 6 mm mild steel stirrups which spaced at 100 mm. Dimension of concrete blocks were 250 mm x 250 mm x **195 mm (390 mm for long embedment), cast with normal concrete (NC) and HPFRCC. Table I provides a summary of the test program. A total of 12 specimens were tested.

B. Materials

The normal concrete achieved compressive strength of 31.8 MPa from 28 days cylinder test and its tensile splitting was 3.92 MPa. HPFRCC was made of 60% of groundground-granulated blast-furnace slag (GGBS) as cement replacement, Ordinary Portland Cement (OPC), Silica Sand (ratio is 0.2 relatively to binder), Polyvinyl Alcohol (PVA) fiber (2% in volume fraction), water (ratio is 0.27 relatively to binder) and superplasticizer. Direct tensile test has been conducted after 28 days of curing. Tensile strength of 3.5 MPa was obtained and tensile strain capacity was 0.75%. Compressive strength of HPFRCC was 53.2 MPa from test at 28 days. Stress-strain relationship obtained from tensile test of the bar is shown in Fig. 2. Table II provides properties the bar.

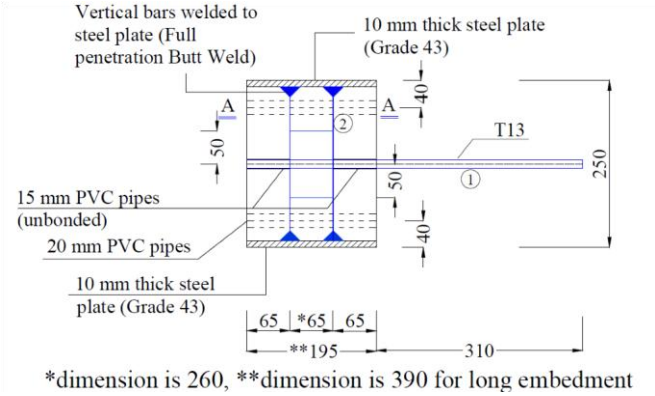

Fig. 1 Details of test specimens

TABLE I
SUMMARY OF TEST PROGRAM

Type of embedment	Material	Number of specimens
Short	NC	
Short	HPFRCC	
Long	NC	
Long	HPFRCC	

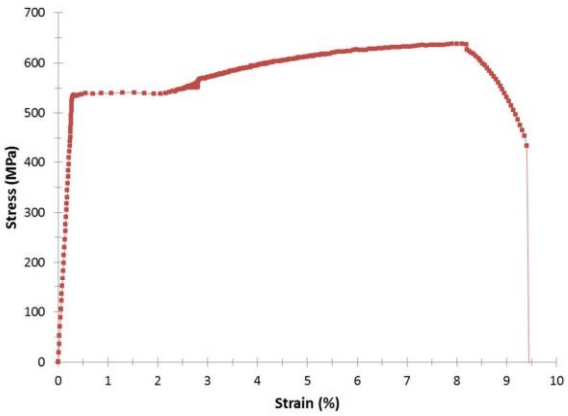

Fig. 2 Stress-strain relationship for T13

TABLE II
PROPERTIES OF BAR

Elastic Modulus	163600 MPa
Yield Strength	MPa
Ultimate Strength	MPa
Yield Stain	
0.33%	
Initial Hardening Stain	2.18%
Fracture Strain	9.40%

C. Test Set-up and Instrumentation

Fig. 3 shows the test set-up and Instron testing machine 200 tons capacity. This set-up was designed to allow the bar to be pulled upwards; lower end of the concrete block was fixed through the use of steel plate connection. The bar was gripped onto the jaw at the top while steel plate was gripped onto the lower jaw. A displacement control loading was utilized throughout the test. For long embedment specimens, a loading rate of 0.5 mm/min was imposed during elastic stage and it increased to 2 mm/min during post-yielding stage. On the hand, a constant loading rate of 2 mm/min was applied for embedment specimens throughout the test. All specimens excessively mounted with LVDTs for measuring bar slip as shown in Fig. 3. For long embedment specimens, post-yield strain gauges were installed along the embedment length to obtain strain profile. A groove of 4.5 mm width x 2.5 mm x 250 mm length was cut on both longitudinal ribs of the bar strain-gauging work. Layout of strain gauges can be seen in Fig. 4.

Fig. 3 Test set-up

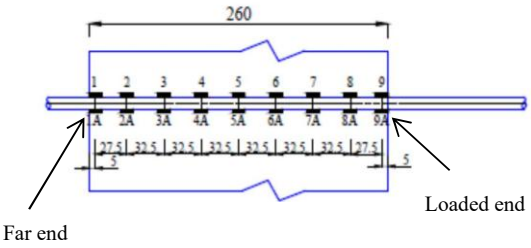

Fig. 4 Layout of strain gauges

III. TEST RESULTS

A. Short Embedment Specimens

Bond stress-slip relationships were deduced by taking applied forces at slip value recorded from LVDTs. The local bond stress at any load level was determined using:

$$\tau = \frac{F}{\pi . d_b . l_e} \quad (1)$$

where F is the applied force; d_b is the bar diameter; and l_e is embedment length. Due to sufficient cover and confining reinforcement, splitting failure was not occurred. All failed by pull-out of the rebar from concrete or HFFRCC at bar stress well below the yield stress of bar. For comparison purpose, all the bond stress were normalized by multiplying bond stress

calculated in equation 1 with $(30/f_c')^{1/2}$. The bond stress versus slip relations for NC specimens and HPFRCC specimens are shown in Fig. 5. Model code 2010 (MC 2010) was incorporated for justification of the test results. Generally NC shows a good agreement with MC 2010 while HPFRCC exhibited better bond behavior. HPFRCC achieved maximum bond strength of 22 MPa, which was almost 50% of increment as compared to MC 2010. Besides, HPFRCC are able to maintain this bond strength through a larger slip range (1.5 to 6 mm). After this, bond strength started to deteriorate for about 30% and it leveled off at a slip of 10 mm. This shows ductile behavior of HPFRCC in bond-slip, the presence of fibers in bridging crack helps to remain greater residual bond strength as compared to NC. Fig. 6 shows the ascending of bond-slip relation. It can be seen that stiffness of HPFRCC was greater than NC; it is because HPFRCC itself has a confining effect in avoiding splitting cracks under the same confining reinforcement and concrete cover. Due to the good confinement in HPFRCC, the load can be increased further until achieving maximum bond resistance.

Fig. 6 Bond stress-slip response (ascending branch)

B. Long Embedment Specimens

For long embedment specimens, all bars were failed by fracture as shown in Fig. 7. The fracture length is about 390 mm measured from the left.

Stage	Justification	Remark
	One-quarter of bar yield load	Yield load
	Half of bar yield load	Yield load
	Three-quarter of bar yield load	Yield load
	Strain ≥ bar yield strain (3300 micro strain)	Yield strain
	Strain ≥ bar hardening strain (21800 micro strain)	Initial Hardening strain

Fig. 7 Fracture of bars

The load versus displacement for each specimen is given in Fig. 8. The maximum load capacity for both NC and HPFRCC are almost similar (72-74 kN), but they showed an obvious difference in terms of maximum displacement. The maximum average displacement for NC and HPFRCC was 12.91 and 9.75 mm respectively. It indicating that bar embedded in the HPFRCC blocks exhibited early fracture relative to NC. At the initial stage (prior to yielding), smaller displacements were recorded in HPFRCC. It was because the transverse cracks formed in the concrete were bridged by fibers. A lower load is being transferred to the bar which induced smaller strain differences between bar and matrix.

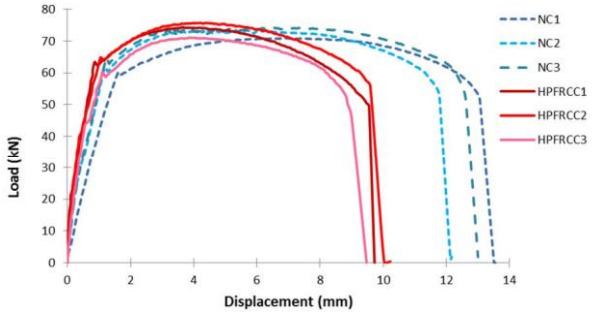

Fig. 8 Load-displacement for long embedment specimens

1. Distribution of Strain, Slip, Bar Stress and Bond Stress

The measured strain was derived from the average value of two strain gauges installed at interval of 2.5 d_b as shown in Fig. 4. Seven stages of strain reading were recorded, based on the result of bar stress-strain curve as indicated in Table III. For the purpose of comparison and due to the difficulties of obtaining strain gauge reading during post-yield, the chosen last stage of strain reading was 55000 micro strain for both type of materials.

The strain distribution for NC and HPFRCC are shown in Figs. 9 and 10. Prior to yielding, strain recorded at the loaded end in HPFRCC was higher than in NC under constant loads (F1 to F3). However, after yielding stage, while strain readings at the loaded end (x = 250 mm) for NC and HPFRCC were in a similar range, a greater strain was recorded at distance x = 222.5 mm in NC as compared to HPFRCC. This implies that yielding of this location was delay in HPFRCC. Smaller slip will be resulted and inelastic length, which the bond reduction occurs, will be shorter.

Strain in between 5 & 7	Hardening Strain
Maximum strain which is recorded by strain gauge (no more than 82000 micro strain)	Hardening Strain

TABLE III
STAGES OF STRAIN READING

(b) All stages

Fig. 10 Strain distribution of HPFRCC

The slip along the bar can be calculated by taking the summation of the integration of strain plot from the free end to the point of concerned. The free end slip is always zero if the embedment is sufficiently long and this is applicable in this experiment. Equation (2) was used for the slip determination.

$$s = \int_0^x \varepsilon dx \quad (2)$$

where S is the slip; and ε is the average strain of the bar. The calculated slip along the bar is shown in Figs. 11 and 12. Generally the total slip at the loaded end in HPFRCC was reduced 40% as compared to NC. The slip value at distance x = 222.5 mm during load stage 6 in NC was about twice of the slip calculated in HPFRCC as the yielding strain has been attained in NC.

The bar stress distribution was determined based on (3) and (4) as:

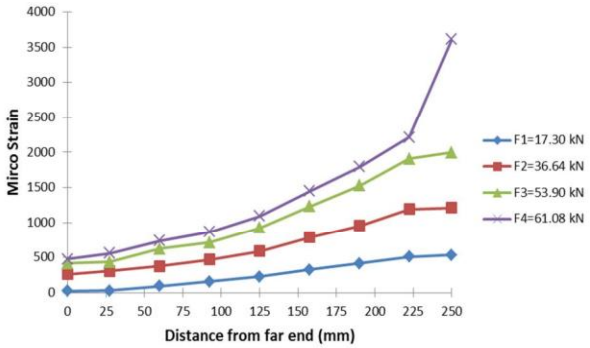

(a) Up to yielding stage

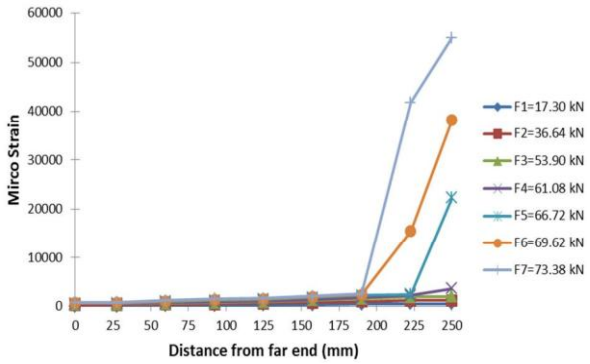

(b) All stages

Fig. 9 Strain distribution of NC

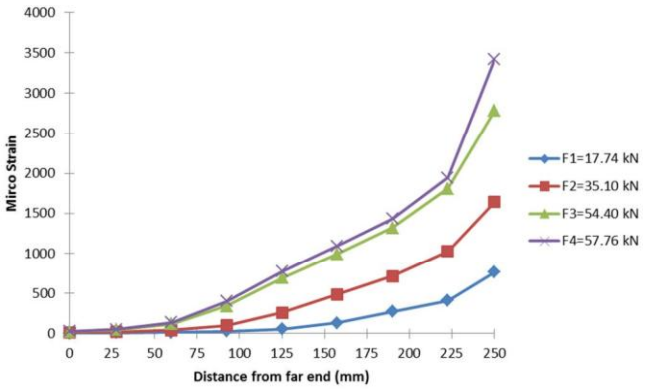

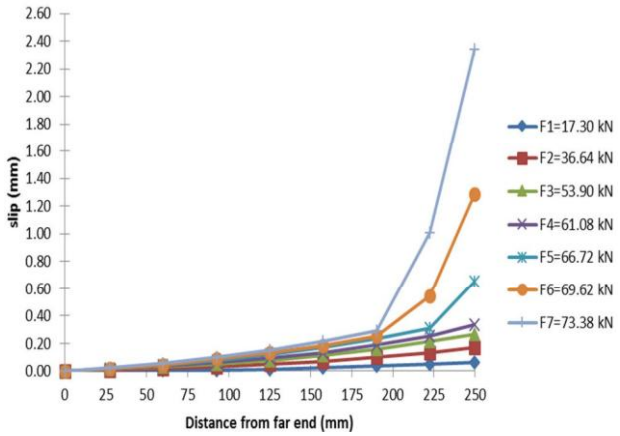

Fig. 11 Slip distribution of NC

(a) Up to yielding stage

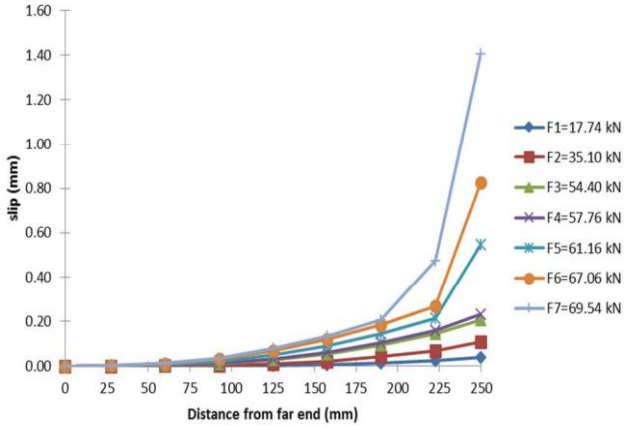

Fig. 12 Slip distribution of HPFRCC

$$\sigma = 163600\,\varepsilon \quad (for \varepsilon \le 0.33\%) \tag{3}$$

$$\sigma = \quad + \quad \varepsilon \quad (for\ 0.33\% \le \varepsilon \le 8.2\%) \tag{4}$$

where σ is the bar stress. Figs. 13 and 14 give the distribution of bar stress. Compared to NC, bar stress at the far end in HPFRCC was generally very small due to smaller strain reading at that particular point. However, bar stress value at the loaded end was slightly higher prior yielding stage in HPFRCC as there was a jumping of the bar stress from $x =$ 222.5 mm to $x = 250$ mm. This phenomenon induced an increasing of bond stress as shown in Fig. 16.

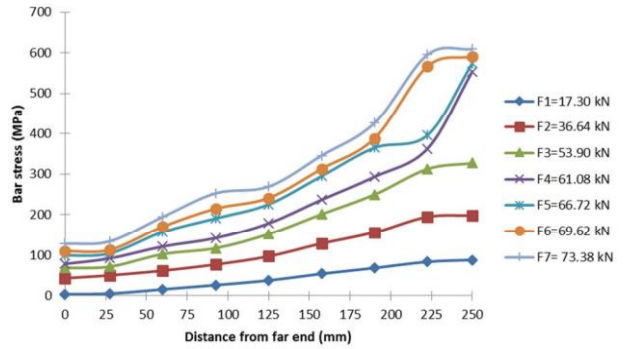

Fig. 13 Bar stress distribution of NC

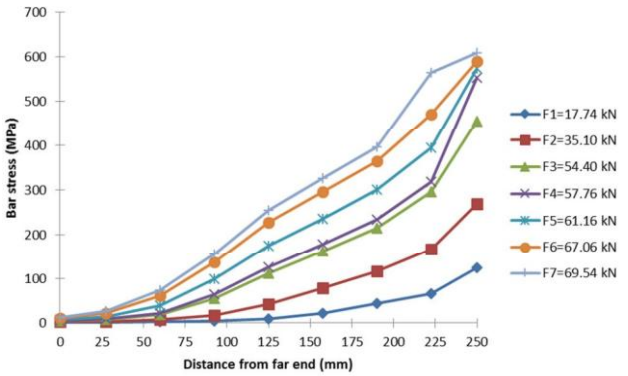

Fig. 14 Bar stress distribution of HPFRCC

The local bond stress at any points along the bar was proportional to the slope of the bar stress distribution, it can be determined by using (5):

$$\tau = \frac{d_b}{4} \cdot \frac{d\sigma}{dx} \tag{5}$$

Bond stress distribution along bar can be found in Figs. 15 and 16. At loaded end, bond stress was reduced significantly during final stages (strain hardening stages). However, this reduction was delayed in HPFRCC as compared to NC. As can be seen, the dropping of bond stress in NC was initiated on stage 6 and above, while in HPFRCC it occurred only during stage 7.

2. Visual Observation of Concrete Crack

In this test, splitting failure was deliberately to be avoided by embedding bar in massive concrete block. Therefore, tensile stress had yet to reach to the outer concrete when fracture of bar occurred. Only a small zone of splitting cracks in the shape of cone were formed on the pulling face in NC specimens but it was not observed in HPFRCC specimens as sho wn in Fig. 17.

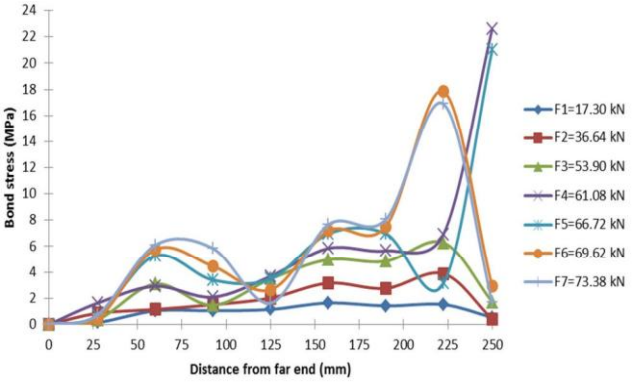

Fig. 15 Bond stress distribution of NC

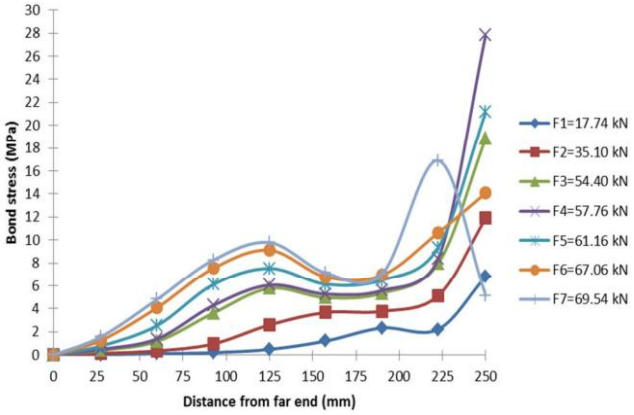

Fig. 16 Bond stress distribution of HPFRCC

(a) NC (b) HPFRCC

Fig. 17 Visual observation after test

IV. CONCLUSIONS

For short embedment, all specimens have failed by pull-out of the bar from concrete blocks. The local bond stress-slip relationship obtained from this test was comparable to MC 2010. HPFRCC showed enhancement of bond strength up to 50% and more ductile of this behavior as compared to NC. The ultimate frictional bond resistance for HPFRCC was about twice of NC; due to presence of fiber that bridging craIcnk asl. l long embedment specimens, bars were fractured at the end of the test. The distribution of strain, slip, bar stress and bond stress were plotted, but not up to final failure stage since reading of strain gauge was not valid. For both NC and HPFRCC, after bar yielded at a location along the bar, the strain at that location dramatically jumped up during the next stage (initial strain hardening). Yielding at the location next to loaded end has been delayed in HPFRCC if compared to NC; this caused the smaller amount of total slip at loaded end. The bond stress dropped significantly at a location during postyield stages, as yielding of bar was attained at the point before. Similarly, this dropping was on hold for HPFRCC. Therefore, test results presented here has demonstrated that HPFRCC able to improve bond-slip behavior for the case of bar anchored in beam-column joints subjected to seismic loading.

REFERENCES

[1] H. Fukuyama, Y. Sato, V. C. Li, Y. Matsuzaki, and H. Mihashi, "Ductile engineered cementitious composite elements for seismic structural application," *12th World Conf. on Earthquake Engineering,* Auckland, New Zealand, 2000, p. 1672.

[2] H. Fukuyama, and H. Suwada, "Experimental response of HPFRCC dampers for Structural Control," *Journal of Advanced Concrete Technology,* vol. 1, pp. 317-326, 2003.

[3] G. Fischer, and V. C. Li, "Effect of matrix ductility on deformation behavior of steel-reinforced ECC flexural members under reversed loading conditions," *ACI Structural Journal,* vol. 99(6), pp. 781-790, 2002.

[4] R. Eligehausen, E. P. Popov, and V. V. Bertero, "Local bond stress-slip relationships of deformed bars under generalized excitations," *Report No. UCB/EERC-83/2,* Earthquake Engineering Research Center, College of Engineering, University of California, Berkeley, 1983.

[5] CEB-FIP, *Fib Model Code for Concrete Structures 2010*. International Federation for Structural Concrete, 2013.

[6] H. Shima, L. L. Chou, and H. Okamura, "Bond characteristics in postyield range of deformed bars," *Concrete Library of Japan Society of Civil Engineers,* No. 10, pp. 113-124, Dec. 1987.

[7] S. Viwathanatepa, E. P. Popov, and V. V. Bertero, "Effects of generalized loadings on bond of reinforcement bars embedded in confined concrete blocks," *Report No. UCB/EERC-79/22,* Earthquake Engineering Research Center, College of Engineering, University of California, Berkeley, 1979.

[8] T. Kanakubo, and H. Hosoya, "Bond splitting strength of reinforced strain-hardening cement composite elements with small bar spacing," *ACI Structural Journal,* vol. 112(17), pp. 189-198, 2015.

[9] K. Asano, and T. Kanakubo, "Study on size effect in bond splitting behaviour of ECC," *HPFRCC 6,* Rilem, pp. 137-144, 2012.

[10] D. M. Moreno, W. Trono, G. Jen, C. Ostertag, and S. L. Billington, "Tension stiffening in reinforced high performance fiber reinforced cement-based composite," *Cement & Concrete Composite,* vol. 50, pp.